

Growth mechanism and properties of ZnO nanorods synthesized by plasma-enhanced chemical vapor deposition

Xiang Liu, Xiaohua Wu, Hui Cao, and R. P. H. Chang
Materials Research Center, Northwestern University, Evanston, Illinois 60208

(Received 18 September 2003; accepted 17 December 2003)

Uniformly distributed ZnO nanorods have been grown by plasma-enhanced chemical vapor deposition using a two-step process. By controlling the oxygen content in the gas mixture during the nucleation and growth steps, no catalyst is required for the formation of ZnO nanorods. High-resolution transmission electron microscopy studies show that ZnO nanorods are single crystals and that they grow along the c axis of the crystal plane. Alignment of these nanorods with respect to the substrates depends on the lattice mismatch between ZnO and the substrate, the surface electric field, and the amount of defects in the starting nuclei. Room-temperature photoluminescence measurements of these ZnO nanorods have shown ultraviolet peaks at 380 nm with a full width at half-maximum of 106 meV, which are comparable to those found in high-quality ZnO films. Photoluminescence measurements of annealed ZnO nanorods in hydrogen and oxygen atmospheres indicate that the origins of green emission are oxygen vacancies and zinc interstitials, while oxygen interstitials are responsible for the orange-red emission. A mechanism for the nanorod growth is proposed. © 2004 American Institute of Physics. [DOI: 10.1063/1.1646440]

I. INTRODUCTION

As a wide-bandgap ($E_g = 3.37$ eV) semiconductor material, ZnO has attracted much interest in recent years due to its potential applications in optoelectronic devices, such as short-wavelength lasers and light-emitting diodes. Molecular-beam epitaxy (MBE), pulsed-laser deposition (PLD), and chemical vapor deposition are among the most commonly used techniques for ZnO film preparation. While most of the efforts have been focused on the growth of high-quality epitaxial ZnO thin films, few reports have been published on the synthesis of ZnO nanorods and nanowires.

To date, studies of semiconductor nanorods, including Si, Ge, GaAs, GaN, and InP, have been reported.¹⁻⁵ One-dimensional nanostructures of ZnO have received special attention recently due to their unique properties. ZnO is a compound semiconductor with a high exciton binding energy of 60 meV, which is significantly larger than other materials commonly used for blue-green light-emitting devices, such as ZnSe (22 meV) and GaN (25 meV). As reported by Cao *et al.*, ZnO nanocrystalline powders and thin films have shown to exhibit room-temperature UV lasing properties.^{6,7} In addition, one-dimensional semiconductors can be utilized as components in nanometer-scale optoelectronic devices. The quantum size effects associated with the low-dimensional nanostructures would enhance radiative recombination because they can increase the density of states at the band edges and confine the carriers.⁸ For example, electrically driven, single-nanowire lasers have been realized by fabricating heterojunctions between CdS nanowires and Si substrates.⁹ For both scientific understanding and potential applications, it is necessary to study the growth mechanism and properties of ZnO nanorods.

For most reports on ZnO nanorods or nanowires growth, the vapor-liquid-solid (VLS) process has been used. In this

case, gold (Au) nanoparticles are used as catalysts to grow ZnO nanorods. However, there are some apparent drawbacks in the VLS growth technique. It requires a very high growth temperature up to 925 °C so that Zn vapor can be dissolved into a Au catalyst to form an alloy droplet.¹⁰ After saturation, Zn precipitates out from the droplet and is oxidized as ZnO nanorods grow. The other intrinsic feature of the VLS growth method is that at the tips of the ZnO nanorods there are always impurity particles that could be undesirable for device fabrication. Park *et al.* have reported ZnO nanorod growth with a low-temperature seed layer by metalorganic vapor-phase epitaxy (MOVPE).¹¹ However, no growth mechanism was investigated.

In this work, vertically well-aligned ZnO nanorods are grown by plasma-enhanced chemical vapor deposition (PECVD) without any catalyst. The growth is carried out in a two-step process by changing the oxygen concentration in the gas mixture. The length and diameter of ZnO nanorods are highly uniform. The areal density of nanorods can be controlled by a two-step growth process. The dependence of nanorod growth on different substrates, surface electric field, and the property of ZnO seed nuclei are studied. A growth mechanism is also proposed.

II. EXPERIMENTAL PROCEDURE

ZnO nanorods are grown on c -plane sapphire, (111)-textured platinum (Pt) film on SiO₂/Si, and Si (100) substrates to study the effects of different templates for nanorod growth. Diethylzinc (DEZn) and oxygen gas are used as precursors for zinc and oxygen, respectively. Nanorod growth is carried out in a pulsed organometallic-beam epitaxy system.¹² During deposition, DEZn precursor is kept in a bubbler cooled to -26 °C and transported into the chamber by helium gas flowing at ~1 sccm. Oxygen gas is introduced

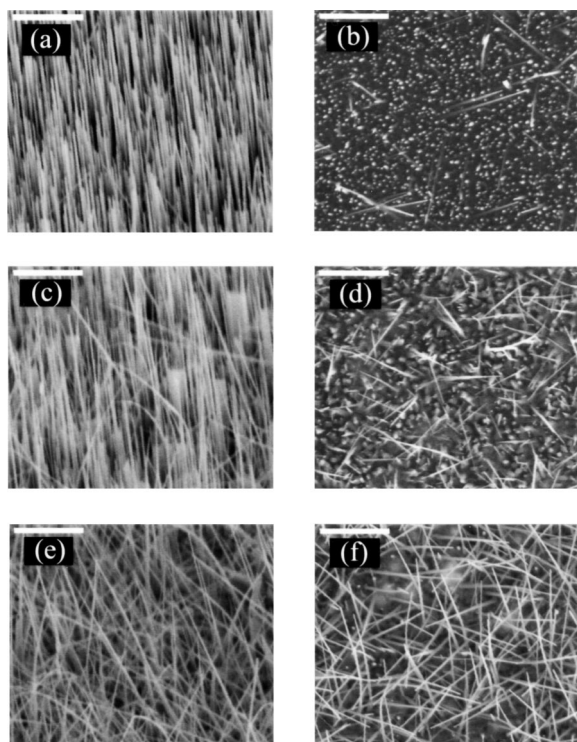


FIG. 1. ZnO nanorods grown on different substrates in plasma. (a) and (b) are 60° tilted view and top view respectively, on *c*-plane sapphire; (c) and (d) are 60° tilted view and top view, respectively, on (111)-textured Pt film; (e) and (f) are 60° tilted view and top view, respectively, on Si substrates. (Scale bars are 1 μm .)

separately into the reaction chamber. All gas flows are controlled by mass flow meter controllers. A microwave plasma is maintained in the chamber during growth, with chamber pressures in the range of 3 to 20 mTorr. Substrates are heated to 700 °C. At the beginning of the growth, a short nucleation process between 30 to 120 s is carried out by pulsing DEZn vapor onto the substrates that are immersed in a plasma with 90% oxygen in helium. The effects of different temperatures and oxygen concentrations on the nucleation process are studied. Following the nucleation step, ZnO nanorods are grown on the nuclei under continuous flow of Zn precursor in a plasma with 20% oxygen in helium. Morphology and structural properties of nanorods are studied by transmission electron microscopy (TEM), scanning electron microscopy (SEM), and x-ray diffraction (XRD), respectively. XRD data are obtained with Cu $K_{\alpha 1}$ radiation. Photoluminescence (PL) measurements on ZnO nanorods are performed with a He-Cd cw laser ($\lambda=325$ nm) at room temperature.

III. RESULTS

When utilizing the two-step growth technique, ZnO nanorods can be grown on different kinds of substrates, as shown in SEM micrographs taken by Hitachi S-4500 field-emission microscope (see Fig. 1). On sapphire and Pt surfaces, the nanorods are well aligned vertically, while on Si substrates they are randomly oriented. The diameters of ZnO nanorods can vary between 20 to 75 nm depending on processing parameters and the lengths can be as long as 2 μm . By changing the nucleation time, the areal density of well-

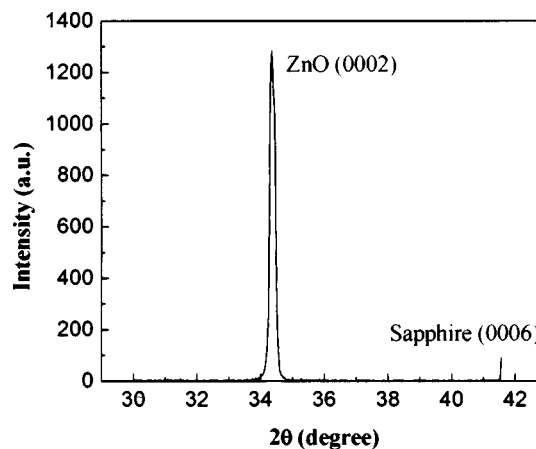


FIG. 2. XRD θ - 2θ scan of ZnO nanorods on *c*-plane sapphire.

aligned ZnO nanorods on sapphire can be varied between $\sim 10^8$ and $\sim 10^{10}/\text{cm}^2$. The XRD θ - 2θ scan data show that, for well-aligned nanorods on sapphire and Pt, only ZnO (000 l) peaks are present (See Fig. 2). The full width at half-maximum (FWHM) of XRD ω rocking curves of ZnO (0002) peaks on sapphire and Pt are 0.6° and 2.3°, respectively. This result suggests that ZnO nanorods are growing along the *c* axis and that they are perpendicular to the surface of sapphire and Pt substrates with fairly small deviation.

High-resolution TEM (HRTEM) micrographs are taken by Hitachi HF-2000 field-emission microscope. Figure 3 shows that ZnO nanorods are high-quality single crystals without visible defects within the area of observation. The electron diffraction pattern, as shown in the inset of Fig. 3, clearly demonstrates that the ZnO nanorods grow as a single crystal along the *c* axis, which is consistent with the XRD data.

PL results are shown in Fig. 4. For ZnO nanorods grown on sapphire, there is only a narrow UV peak at around 380 nm. No other peaks are present in the PL spectrum for ZnO nanorods on sapphire. However, the PL spectra for those grown on Pt and Si, especially for Si substrates, show broad peaks centering at around 520 nm in addition to the UV band. Emission at 630 nm emerges in PL spectra after annealing.

IV. DISCUSSION

A. Two-step growth mechanism

A two-step growth method has been developed to grow ZnO nanorods by changing the oxygen content in gas mixture during nucleation and growth steps. This is based on our systematic studies of ZnO nucleation and growth under different conditions. Due to the large lattice mismatch ($\sim 18\%$) between ZnO and sapphire, the nucleation of ZnO on sapphire follows the three-dimensional island growth; that is, the Volmer-Weber mode, as reported by Yamauchi *et al.* in their observation of plasma-assisted epitaxial growth of ZnO on sapphire.^{13,14} At high temperature, the nucleation of ZnO islands on the surface of substrates depends strongly on the amount of active oxygen. When grown entirely in 90% oxygen plasma, ZnO has a high nucleation density and forms

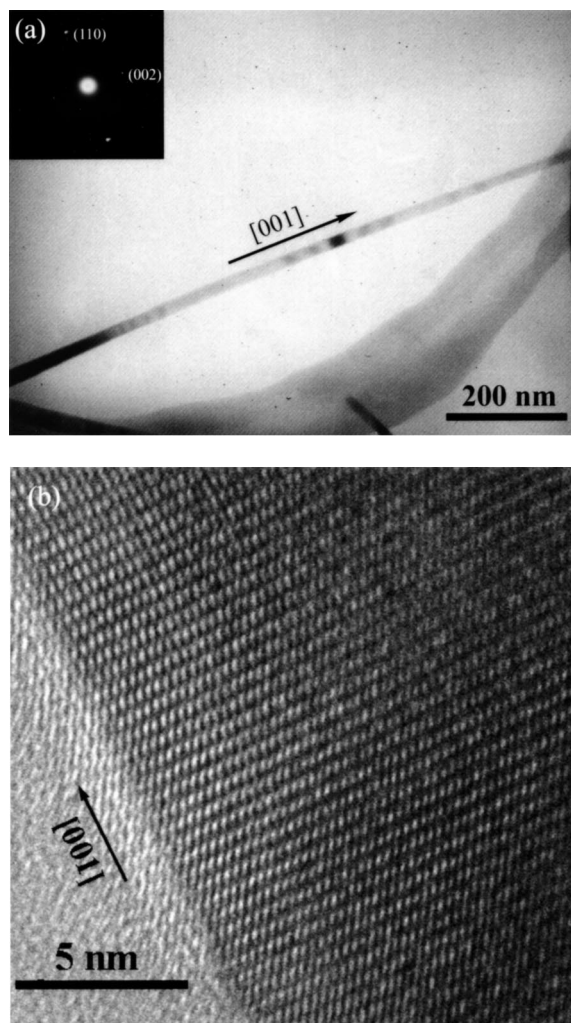


FIG. 3. (a) TEM micrograph of ZnO nanorods. Inset is the electron diffraction pattern of the nanorod. (b) HRTEM of a ZnO nanorod.

continuous thin films with columnar-shaped grains on sapphire substrates at around 700 °C, as shown in SEM image in Fig. 5(a). No nanorods can be found in this case. On the other hand, when oxygen content in the gas mixture is reduced, it is difficult to nucleate ZnO on the substrates. According to nucleation theory, nucleation density can be described by the following equation:¹⁵

$$N = A \exp(-\Delta G^*/RT),$$

where N is nucleation density, ΔG^* is activation energy of nucleation, which is composed of volume free energy ΔG_V and surface free energy ΔG_S , T is growth temperature, and A is a constant. For the chemical reaction of $\text{DEZn} + \text{O}_2 \rightarrow \text{ZnO} + \text{H}_2\text{O} + \text{CO}_2$, as $\Delta G_V \propto -\ln P(\text{O}_2)$, the free energy change per unit volume ΔG_V increases with decreasing concentration of oxygen. Thus, at low oxygen concentration, the activation energy of nucleation is higher, which makes nucleation of ZnO more difficult. As seen in Fig. 5(b), when ZnO growth is carried out entirely in 20% oxygen plasma, almost no ZnO is grown, except for a few large clusters sparsely located on the substrates, possibly from some dust contamination. To further confirm this observation, we dispersed ZnO nanoparticles on sapphire substrates and tried to grow

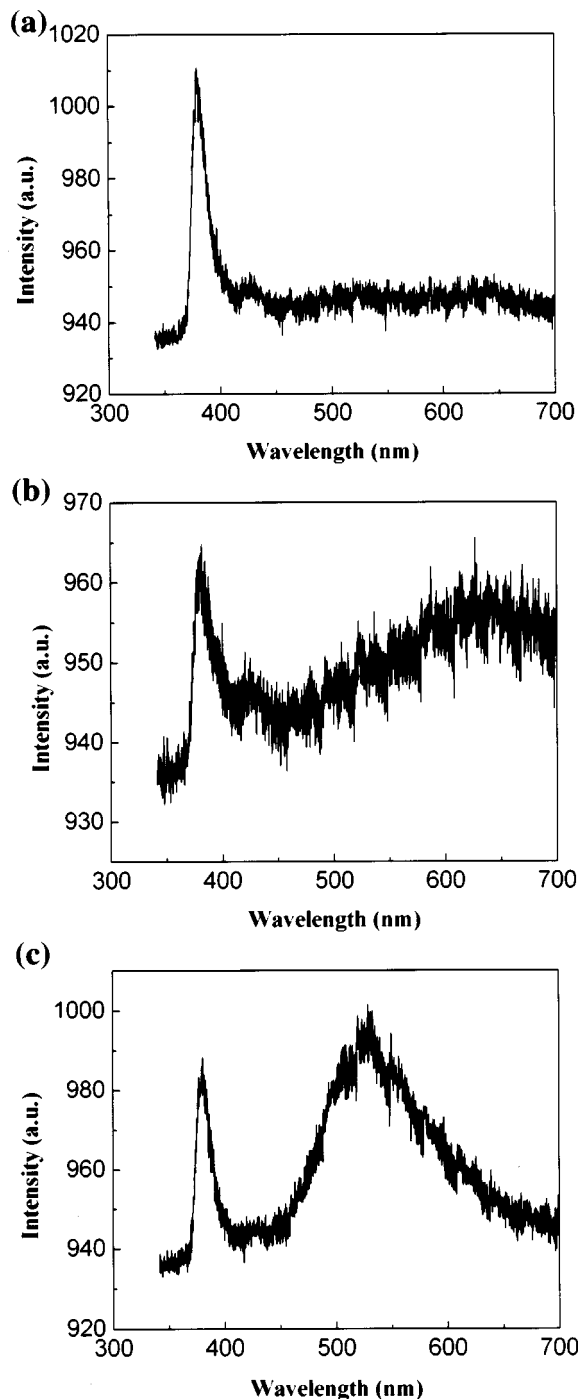


FIG. 4. PL spectra of ZnO nanorods on (a) sapphire, (b) Pt, and (c) Si.

nanorods in a 20% oxygen plasma environment. ZnO nanorods are found to grow only from the nanoparticles that serve as seeds for the growth (see Fig. 6). This indicates that, under the low oxygen content condition, ZnO growth is facilitated with pre-existing seeds, while nucleation on bare substrate is difficult. Based on these observations, we have developed a two-step growth method for ZnO nanorods. In the nucleation step, by pulsing the DEZn into 90% oxygen plasma, sufficient active oxygen species are provided around the substrates so that the Zn precursor can react with oxygen on the

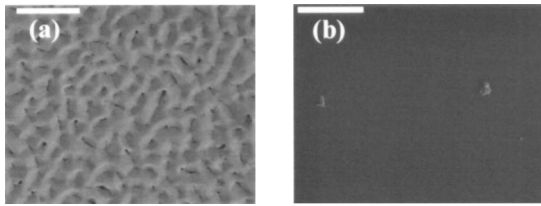


FIG. 5. (a) ZnO grown on sapphire in 90% oxygen. (b) No ZnO can be grown on sapphire in 20% oxygen without nucleation layer. (Scale bars are 1 μm .)

surface and can be fully oxidized. Under this condition, ZnO can nucleate on the sapphire surface. Similarly, ZnO nucleates on textured Pt films and Si substrates.

After the nucleation process, oxygen flow is reduced to 20% of the gas mixture, and continuous growth of ZnO is carried out in oxygen and helium plasma for 1 h. As the amount of oxygen is reduced, additional nucleation of ZnO on the bare substrate surface is difficult, because sufficient oxygen is required for nucleation, as discussed before. Under this oxygen-deficient condition, ZnO will grow preferentially on the pre-existing ZnO sites that have been formed during the first step. In addition, due to the faster vertical growth rate along the c axis compared to the lateral directions, rod-shaped ZnO crystals are developed. We find that the percentage of oxygen in the total gas mixture is critical for growth of nanorods. When 5% or 10% oxygen is used for growth, no ZnO nanorods are observed. In these cases, oxygen content is so low that growth of ZnO is extremely slow or cannot

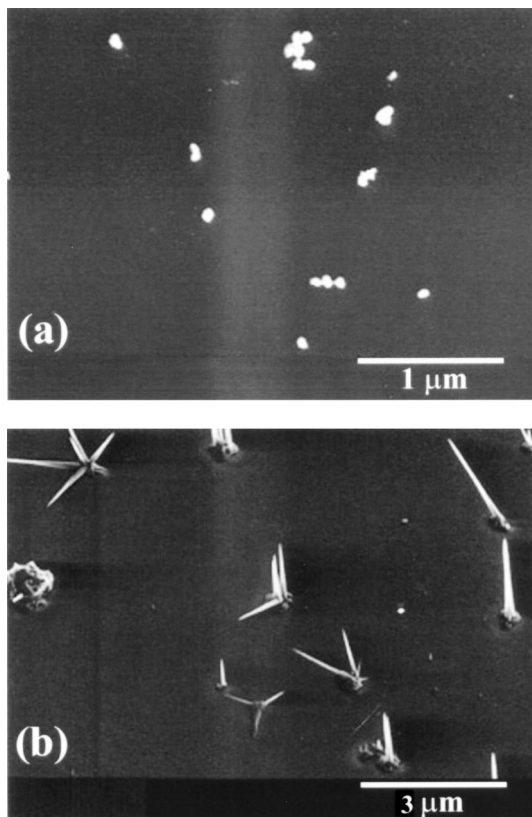


FIG. 6. ZnO nanorod growth using ZnO nanoparticles as seeds. (a) ZnO nanoparticles before growth. (b) ZnO nanorods after growth.

take place at all. By controlling the amount of oxygen in gas mixture, we have grown ZnO nanorods by this two-step growth method.

B. Alignment of ZnO nanorods

1. Effect of different substrates

For many nanorod applications, such as field emission, it is important to control the alignment of nanorods. Three kinds of substrates— c -plane sapphire, (111)-textured Pt layer on silicon, and (100) silicon—are used for ZnO nanorod growth in plasma. These substrates are chosen for their different compatibilities with ZnO crystal. Due to the epitaxial relation between ZnO and sapphire, ZnO prefers to grow along the c axis on c -plane sapphire; that is, ZnO [0001] parallel to sapphire [0001] as confirmed by XRD data. The template provided by sapphire substrates enables all the ZnO nanorods to be well-aligned along the same direction. Park *et al.* also reported similar aligned ZnO nanorods on c -plane sapphire grown by MOVPE.¹¹ For (111)-textured Pt film, having fcc structure, the (111) planes of Pt surface have a hexagonal two-dimensional lattice, and can also serve as templates for the close-packed basal plane of ZnO. Therefore, ZnO nanorods can also grow in alignment along the c axis on (111)-textured Pt films. However, on Si (100) substrates, ZnO nuclei are randomly oriented due to lack of lattice compatibility between ZnO and the Si (100) surface. As a result, the alignment of ZnO nanorods on Si (100) is quite different from that on sapphire or Pt. They are totally randomly oriented, which can be seen in the SEM pictures in Fig. 1. These results show that lattice matching between ZnO nanorods and substrates plays an important role in the self-alignment of ZnO nanorods.

2. Effect of electric field

The sheath electric field between the plasma and the substrate surface contributes greatly to the preferential growth along the c axis of ZnO nanorods by attracting the charged particles to the protruding tips. For microwave oxygen plasma at a pressure of 3 mTorr, the self-bias potential on the substrate surface is measured by Langmuir probe to be around 15 V. This potential is dropped across the plasma sheath estimated to be 500 μm above substrate surface. Thus, the electric field strength is on the order of 300 V/cm, which is comparable to the electric field strength used to grow aligned carbon nanotubes.¹⁶ Because the self-bias electric field is intrinsically perpendicular to the substrate surface, it helps the ZnO nanorods to grow vertically. To demonstrate the effect of the electric field, we have grown ZnO nanorods without plasma. As shown in Fig. 7, ZnO nanorods grown on c -plane sapphire without plasma are not oriented perpendicular to the substrate surface. However, these nanorods are not randomly oriented either. Instead, they grow at certain tilted angles. According to Fuller's study, this is due to the formation of tetrapod-like junctions of nanorods by twinning on the ZnO (11 $\bar{2}$ 2) plane.¹⁷ Due to the large lattice mismatch between ZnO and sapphire, the density of crystal defects, such as dislocations, is quite high near the ZnO/sapphire interface. When nanorods are grown without

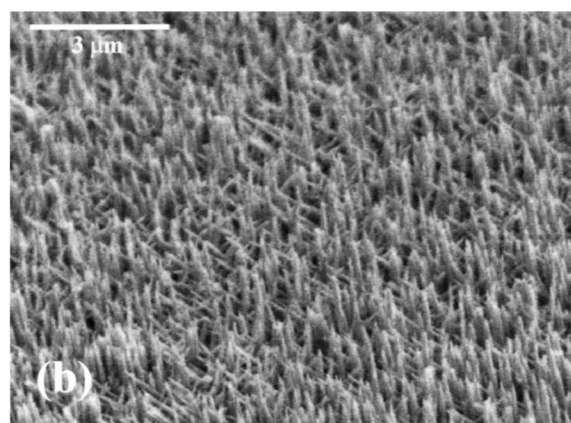
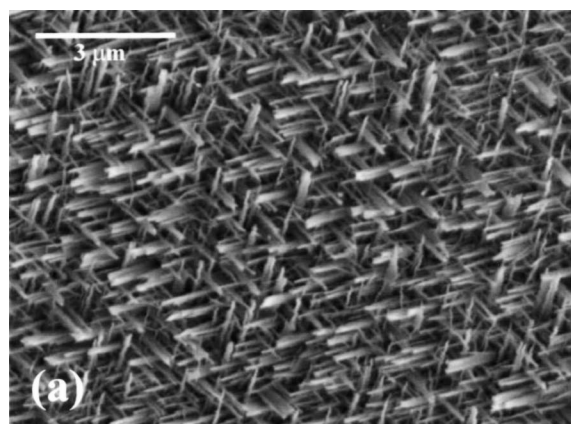


FIG. 7. SEM images of (a) tilted view and (b) top view of ZnO nanorods grown on *c*-plane sapphire without plasma.

plasma, defects in ZnO nuclei can increase the chance of forming tetrapod-like junctions, resulting in tilted nanorods. However, when nanorods are grown with a plasma, they tend to grow along the direction of the electric field. Based on these results, the electric field in the plasma sheath is essential to the control of the orientation of ZnO nanorods in our growth method.

3. Effect of defects in the ZnO nuclei

In the absence of a plasma, oxygen vacancies in ZnO crystal nuclei can exist. We have shown earlier that under the oxygen-deficient condition nanorods grow in tilted directions. To prove such defects have a large effect on the formation of tetrapod-like ZnO nanorods, we have performed the following experiments: after the nucleation step that takes place at a low oxygen pressure around 3 mTorr (same as earlier), the oxygen pressure is increased to 5 Torr and the ZnO nuclei are annealed in this environment for 30 min at 700 °C before the Zn precursor is introduced for nanorod growth. The soaking process drastically reduces the amount of tilted ZnO nanorods. As shown in Fig. 8, most of the nanorods are now aligned vertically to the substrate surface. By annealing the ZnO nuclei at 700 °C in an oxygen environment at higher pressure, defects in the ZnO nuclei are reduced, and thus twinning in ZnO nanorods is also suppressed. Thus, without plasma, higher oxygen pressure is required to grow well-aligned ZnO nanorods. Similar results

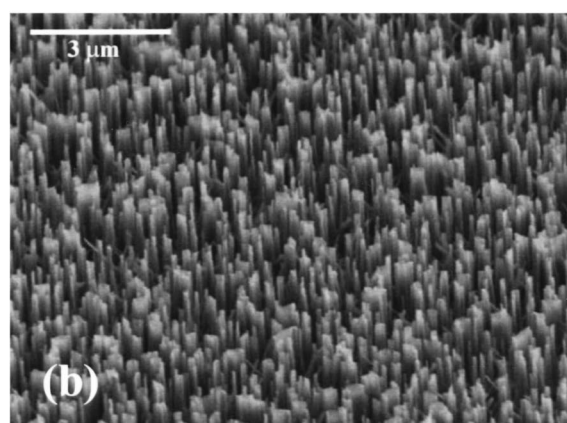
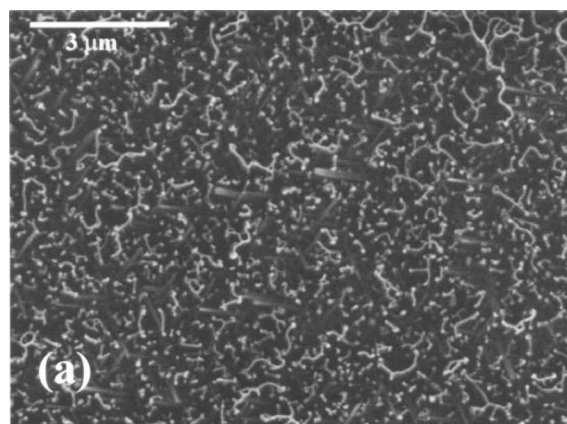


FIG. 8. SEM images of (a) top view and (b) tilted view of ZnO nanorods grown on *c*-plane sapphire without plasma after soaking nuclei in higher oxygen pressure.

have been reported by Park *et al.*¹¹ Tetrapod-like ZnO nanorods are not found in Park's work because they keep the pressure constant and vary the temperature during both seeding and growth stages.

C. Control of nanorod density

For ZnO nanorods grown by the VLS method, a thin film of Au catalyst is deposited on substrates prior to the nanorod growth. Upon heating, the Au layer will turn into high-density nanoparticles. By controlling the thickness of the Au layer and growth temperatures, the areal density of ZnO nanorods density can be changed.

In our two-step approach, instead of Au catalytic particles, there are ZnO island-shaped nuclei on the substrate surfaces after the nucleation step. The areal density of nanorods can be changed by varying the nucleation time. Within a certain time period, the longer the nucleation time, the more ZnO nuclei form on the substrate surface. In this research, the density of ZnO nanorods can be varied between $3.5 \times 10^8 \text{ cm}^{-2}$ and $8.5 \times 10^9 \text{ cm}^{-2}$ on *c*-plane sapphire by changing the net nucleation time between 60 to 120 s, and keeping the growth temperature at 700 °C (see Fig. 9).

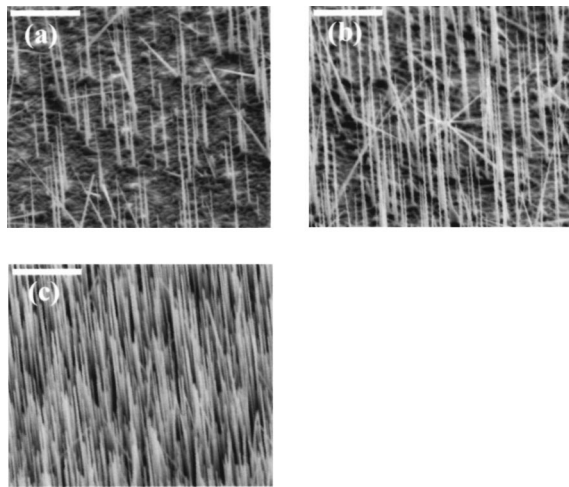


FIG. 9. ZnO nanorods grown on *c*-plane sapphire with different nucleation times and resulting different areal densities. (a) Nucleation time=1 min, nanorod density $\sim 3.5 \times 10^8 \text{ cm}^{-2}$. (b) Nucleation time=1.5 min, nanorod density $\sim 1.5 \times 10^9 \text{ cm}^{-2}$. (c) Nucleation time=2 min, nanorod density $\sim 8.5 \times 10^9 \text{ cm}^{-2}$. (Scale bars are 1 μm .)

D. Optical properties of ZnO nanorods

It is commonly known that the room-temperature PL spectra for ZnO usually show three major peaks: a UV near-band-edge emission peak around 380 nm, a green emission peak around 520 nm, and a red or orange emission around 600 nm.¹⁸ The UV peak is attributed to band-edge emission, while the two broad visible bands are generally attributed to deep-level defects in ZnO crystal, such as vacancies and interstitials of zinc and oxygen. In this work, both the UV and green peaks are present in our PL data. To confirm the origins of the defect peak of ZnO nanorods, samples of ZnO nanorods are annealed in both reducing and oxidizing atmospheres (see Fig. 10). After annealing in 20% hydrogen (in argon) at 400 °C for 30 min, the defect PL peak at 520 nm increases significantly, while UV peak intensity decreases, as seen in Fig. 10(a). On the other hand, after annealing in pure oxygen flow at 400 °C for 30 min, as shown in Fig. 10(b), the defect peak at 520 nm does not change significantly, while the UV emission intensity has substantially decreased. The defect peak at 520 nm is due to oxygen vacancies and zinc interstitials.¹⁹

We can explain our observation as follows: The large surface area of the ZnO nanorods with small diameters form surface states and depletion layers near the nanorod's surface. This plays an important role in the PL process. Close to the surface region, when electrons are excited to the conduction band, they are easily trapped by high-density surface states and are relaxed via a nonradiative process, so that photon emissions can occur only in the central region of the ZnO nanorods, deep from the surface. When ZnO nanorods are annealed in hydrogen atmosphere, more oxygen vacancies and zinc interstitials are created, which increases the emission centers of green peak at 520 nm. At the same time, the free carrier density is also increased in ZnO and therefore reduces the width of depletion region and increases the volume of bulk region where radiative recombination occurs.¹⁹ Consequently the intensity of the green PL peak increases

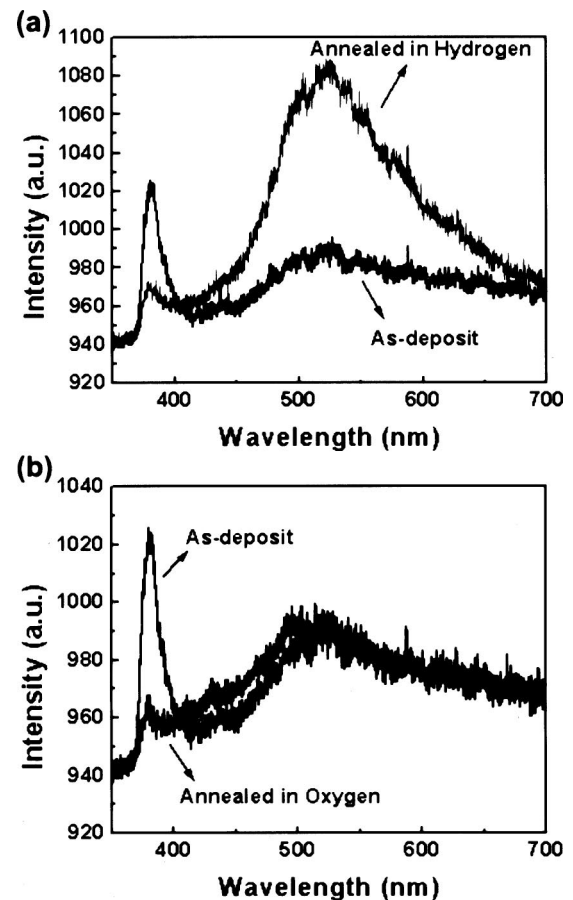


FIG. 10. PL spectra of ZnO nanorods before and after annealing at 400 °C in (a) hydrogen and (b) oxygen.

significantly while the UV emission is suppressed due to large competition from the defect emission. On the other hand, when the ZnO nanorods are annealed in oxygen, some oxygen vacancies are removed and the free carrier density in ZnO decreases, so that the depletion region is widened. The volume of the bulk region is reduced due to effectively reducing the diameters of nanorods. Under this condition, the electrons excited to conduction band will move toward the center bulk region due to enhanced band bending. These electrons are very likely to relax to defect level and then emit green light via radiative recombination. Thus, at the same time, the UV band-edge emission intensity is greatly reduced. We believe that the reduction of emission centers due to oxygen annealing is being compensated by the increase in the number of relaxed electrons from the conduction band to the defect level; thus, the overall PL intensity at 520 nm does not change significantly.

Annealing experiments at even higher temperatures were also performed in both hydrogen and oxygen media. In the hydrogen atmosphere, ZnO nanorods are totally reduced to metallic zinc and evaporated away in 15 min at 550–600 °C. After annealing in oxygen atmosphere for 15 min at 700 °C, the PL peak at 380 nm disappears, and the broad defect emission is enhanced (see Fig. 11). It should be noted that the broad peak becomes obviously asymmetric. This broad band can be deconvoluted into two Gaussian peaks, as shown in Fig. 11(b). One peak is still centered around 520 nm, and the

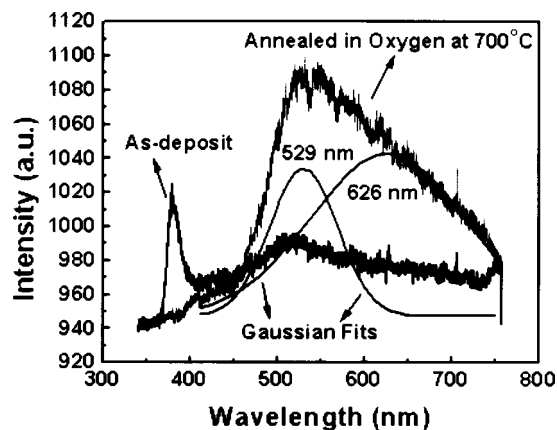


FIG. 11. PL spectra of ZnO nanorods annealed in oxygen at 700 °C. Solid lines are Gaussian fits of the defect emission after annealing.

other peak is centered around 626 nm. This orange-red emission has been found in oxygen-rich ZnO films, and is attributed to oxygen interstitial defects.^{18,20} This implies that when ZnO nanorods are annealed in pure oxygen at high temperature, new defects of oxygen interstitials are created. The effect of increasing oxygen interstitial defects with increasing temperature in PLD-grown ZnO films has also been reported recently.²⁰

Similarly, hydrogen annealing of ZnO films has also been carried out as a comparison. The green defect peak in the PL spectrum of ZnO films does not increase noticeably when the annealing temperatures are below 550 °C. Due to the large surface areas and small diameters of ZnO nanorods, hydrogen diffuses readily into the crystal rods to further remove oxygen from ZnO crystal, thus creating more oxygen vacancies. However, for the case of ZnO films, it takes higher thermal energy for hydrogen to diffuse deep into the film to react with stoichiometric ZnO. The high sensitivity of ZnO nanorods to the gas environment could lead to applications such as sensing.

The ratio of the intensities of UV peak to green peak in spectra of room-temperature PL, shows that under same growth condition, ZnO nanorods grown on sapphire have the highest UV-to-green emission intensity ratio. Those grown on Pt and Si substrates have more pronounced defect emissions. We conclude that epitaxial growth of ZnO on *c*-plane sapphire leads to higher crystallinity and fewer defects, so that it reduces the source of the green emission. In this work, the FWHM of the UV peak in PL spectra of ZnO nanorods on sapphire is 104 meV, which is comparable to high-quality epitaxial films grown by MBE.²¹

V. CONCLUSION

A two-step nucleation and growth method is developed to grow well-aligned ZnO nanorods by PECVD without metallic catalysts. TEM and XRD data show that ZnO nanorods

grow along the *c* axis and are single crystals. PL measurements show only UV emission for ZnO nanorods grown on sapphire substrates, indicating high-quality crystals. Annealing ZnO nanorods in reducing and oxidizing atmosphere at 400 °C changes the intensities of UV and defect peaks in PL spectra, which indicates that the origins of green emission are oxygen vacancies and zinc interstitials. Annealing at higher temperatures reveals that oxygen interstitials are responsible for the orange-red emission. Lattice matching between ZnO and substrates, electric field enhancement, and the amount of defects in the starting nuclei are found to be important to the self-alignment of nanorods. The areal density of ZnO nanorods can be varied by controlling the nucleation time. This can be of great use in future applications such as constructing two-dimensional photonic crystals, in which precise control of nanorod density is needed.

ACKNOWLEDGMENTS

The authors thank Dr. A. Yamilnov for helpful discussion on PL data. We also thank Jun Liu for help on microscopy work. This work is supported in part by the MRSEC program of the National Science Foundation (DMR-0076097), National Science Foundation (ECS-0244457), and NASA under award no. NCC 2-1363.

- ¹J. T. Hu, T. W. Odom, and C. Lieber, *Acc. Chem. Res.* **32**, 435 (1999).
- ²Y. Wu and P. Yang, *Chem. Mater.* **12**, 605 (2000).
- ³M. Yazawa, M. Koguchi, A. Muto, M. Ozawa, and K. Hiruma, *Appl. Phys. Lett.* **61**, 2051 (1992).
- ⁴X. Duan and C. M. Lieber, *J. Am. Chem. Soc.* **122**, 188 (2000).
- ⁵M. S. Gudiksen and C. M. Lieber, *J. Am. Chem. Soc.* **122**, 8801 (2000).
- ⁶H. Cao, Y. G. Zhao, S. T. Ho, E. W. Seelig, Q. H. Wang, and R. P. H. Chang, *Phys. Rev. Lett.* **82**, 2278 (1999).
- ⁷H. Cao, Y. G. Zhao, X. Liu, E. W. Seelig, and R. P. H. Chang, *Appl. Phys. Lett.* **75**, 1213 (1999).
- ⁸M. Huang, S. Mao, H. Feick, H. Yan, Y. Wu, H. Kind, E. Weber, R. Russo, and P. D. Yang, *Science* **292**, 1897 (2001).
- ⁹X. Duan, Y. Huang, R. Agarwal, and C. M. Lieber, *Nature (London)* **421**, 241 (2003).
- ¹⁰M. H. Huang, Y. Y. Wu, H. Feick, N. Tran, E. Weber, and P. D. Yang, *Adv. Mater. (Weinheim, Ger.)* **13**, 113 (2001).
- ¹¹W. I. Park, D. H. Kim, S. W. Jung, and Gyu-Chui Yi, *Appl. Phys. Lett.* **80**, 4232 (2002).
- ¹²S. J. Duray, D. B. Buchholz, S. N. Song, D. S. Richeson, J. B. Ketterson, T. J. Marks, and R. P. H. Chang, *Appl. Phys. Lett.* **59**, 1503 (1991).
- ¹³S. Yamauchi, H. Handa, A. Nagayama, and T. Hariu, *Thin Solid Films* **345**, 12 (1999).
- ¹⁴S. Yamauchi, T. Ashiga, A. Nagayama, and T. Hariu, *J. Cryst. Growth* **214/215**, 63 (2000).
- ¹⁵M. Ohring, in *The Materials Science of Thin Films*, 1st ed. (Academic, London, 1992), p. 42.
- ¹⁶C. Bower, W. Zhu, S. Jin, and O. Zhou, *Appl. Phys. Lett.* **77**, 830 (2000).
- ¹⁷M. L. Fuller, *J. Appl. Phys.* **15**, 164 (1944).
- ¹⁸S. A. Studenikin, N. Golego, and M. Cocivera, *J. Appl. Phys.* **84**, 2287 (1998).
- ¹⁹K. Vanheusden, W. L. Warren, C. H. Seager, D. R. Tallant, and J. A. Voigt, *J. Appl. Phys.* **79**, 7983 (1996).
- ²⁰X. L. Wu, G. G. Siu, C. L. Fu, and H. C. Ong, *Appl. Phys. Lett.* **78**, 2285 (2001).
- ²¹Y. F. Chen, D. M. Bagnall, H. J. Koh, K. T. Park, K. Hiraga, Z. Q. Zhu, and T. Yao, *J. Appl. Phys.* **84**, 3912 (1998).